Synthesis and magnetic properties of $Pr_xCe_{1-x}Fe_2$ compounds

1997 J. Phys.: Condens. Matter 9 9651

(http://iopscience.iop.org/0953-8984/9/44/019)

J. Phys.: Condens. Matter **9** (1997) 9651–9659. Printed in the UK PII: S0953-8984(97)84503-1

Synthesis and magnetic properties of $Pr_xCe_{1-x}Fe_2$ compounds

C C Tang, W S Zhan, Y X Li, D F Chen, J Du, G H Wu, J Y Li and K C Jia

State Key Laboratory for Magnetism, Institute of Physics, Chinese Academy of Sciences, Beijing 100080, People's Republic of China

Received 27 May 1997, in final form 4 August 1997

Abstract. The synthesis and magnetic properties of $Pr_xCe_{1-x}Fe_2$ have been investigated. The formation of $Pr_xCe_{1-x}Fe_2$ is found to depend strongly on annealing temperature. Pure single-phase compound can be synthesized at ambient pressure when $x \leqslant 0.5$. The main phase of the Laves structure can still be observed up to $x = 0.8$. The study of crystalline parameters, magnetic moments and Mössbauer spectra for single-phase $Pr_xCe_{1-x}Fe_2$ is performed. Curie temperature and local Fe magnetic moment increase with the increasing Pr concentration. Extrapolating the trends the spontaneous magnetization and anisotropy constant of $PrFe_2$ are 4.98 μ_B fu^{-1} and 7.3×10^5 J m^{-3} at 1.5 K, respectively. Magnetostriction increases with increasing x and the largest saturation magnetostriction, 200 ppm, is observed for $x = 0.5$. With the increase of Pr concentration, lattice parameter and spontaneous magnetization anomalies exist in a specific range $0.2 < x < 0.5$ that can be attributed to the change of Ce ion valence toward tetravalent.

1. Introduction

A large magnetostriction might be expected in $PrFe_2$ based on the single-ion model prediction [1] and it is a potential candidate for a giant magnetostrictive material. However, previous research indicated that some rare-earth–iron Laves phase compounds RFe_2 (R = La, Pr, Nd, Eu, Yb) [1] had not been synthesized at ambient pressure. This is usually ascribed to the larger atomic radii of rare-earth elements in these compounds than that in other rare-earth–iron compounds. The size factor plays an important role in manufacturing these compounds, called 'size compounds' [2] because the ideal ratio between the two atom radii is about 1.225. For R–Fe systems, this ratio decreases gradually from La to Lu following the trend of the lanthanide contraction, hence the formation of the light-rare-earth–iron Laves phase is more difficult than that of the heavy-rare-earth one. In fact, only the compounds $CeFe_2$ and $SmFe_2$ have been synthesized at ambient pressure so far. The success of the synthesis using a high-pressure technique for (Yb, Nd, Pr)–Fe_2 can be attributed to the reduction of radii of rare-earth ions under pressure [3–5].

However, the formation of two Laves phases, $CeFe_2$ and $YbFe_2$, imply that there might be some other factors affecting the Laves phase construction. For $CeFe_2$ that can be easily synthesized at ambient pressure and with low lattice parameter in comparison to other RFe_2, the Ce 4f electron participates in the construction of the conduction band and mixed-valence behaviour appears; hence the cohesive energy is obviously larger than that of $Ce^{3+}Fe_2$. For $YbFe_2$, the Laves phase formation must be under high pressure although Yb is located on the heavy-rare-earth side. Taking account of Yb $4f^{14}$ configuration, the metallic bond is

0953-8984/97/449651+09$19.50

weak due to the lack of the additional conduction electron and as a result of the small cohesive energy.

The method of melt-spinning and hot-pressing was applied successfully to the synthesis of $(Ce, Pr)Fe_2$, and $(Ce, Nd)Fe_2$ [6]. In the present paper, the traditional method, arc melting with post-annealing under appropriate conditions, was employed to synthesize the $Pr_xCe_{1-x}Fe_2$ compounds. In a wide range $x \leqslant 0.5$ the samples were verified as pure single Laves phase, and the main phase of the Laves structure can still be observed up to $x = 0.8$. The corresponding analysis of the crystalline structure, magnetic properties, magnetostriction and Mössbauer spectra is presented.

2. Experiment

The ingots $Pr_xCe_{1-x}Fe_2$ (x from 0.2 to 1.0) were prepared by arc melting the appropriate amounts of Fe (purity better than 99.9 wt.%) and rare earth (99.95 wt.%) under a purified-argon atmosphere. The relative amount of the rare earth was more than the stoichiometric composition by 10% in order to compensate for the loss of the rare-earth metals during melting. The as-cast ingots were wrapped in tantalum foils and vacuum annealed in sealed quartz capsules. Different annealing temperatures were selected: (1) 850 °C, 3 days, (2) 800 °C, 5 days, and (3) 700 °C, 1 week.

The crystal structure was analysed by x-ray diffraction and lattice parameters were determined by least-squares fit to the x-ray pattern. The magnetization for the single-phase samples was measured by an extracting sample magnetometer at temperatures of 1.5 and 78 K in magnetic fields up to 64 kOe. Curie temperatures were determined by measurements of magnetization as a function of temperature by magnetobalance from room temperature to 700 K in a magnetic field of 500 Oe. Magnetostrictions for the same samples were measured using the strain gauge in applied magnetic fields up 20 kOe at room temperature.

The ^{57}Fe Mössbauer absorption spectra were recorded at a temperature of 78 K using a ^{57}Co source and a constant-acceleration Mössbauer spectrometer. An α-Fe foil was used for the velocity calibration of ^{57}Fe Mössbauer absorption spectra. The absorption spectra were analysed with least-squares computer programs.

3. Results

3.1. Phase analysis

After arc melting, all samples appear multiphase and contain a little α-Fe. Some rare-earth oxide can also be found as the light-rare-earth metal compounds become oxidized easily in the process of manufacturing. The Laves phase is preferable for $x < 0.6$ and is not detected for $x > 0.7$. Low-temperature annealing, for instance 600 °C, does not lead to the occurrence of pure phase [7], so higher temperatures were adopted directly in the experiment.

After annealing at a temperature higher than 800 °C, the phase characteristics for $x \leqslant 0.5$ are almost the same as before annealing. However, only the pure Laves phase occurs after annealing at the temperature 700 °C. The x-ray diffraction spectra for $Pr_{0.5}Ce_{0.5}Fe_2$ at different annealing temperatures are plotted in figure 1. For those samples of Pr concentration $x > 0.5$, the effect of annealing temperature appears to be the opposite to that for samples of $x \leqslant 0.5$ as can be clearly seen from the figure 2, x-ray diffraction spectra of $Pr_{0.7}Ce_{0.3}Fe_2$ at 700, 800 and 850 °C. When the temperature is at 700 or 800 °C, Laves phase structure cannot be detected, but at 850 °C a main phase RFe_2 occurs with a

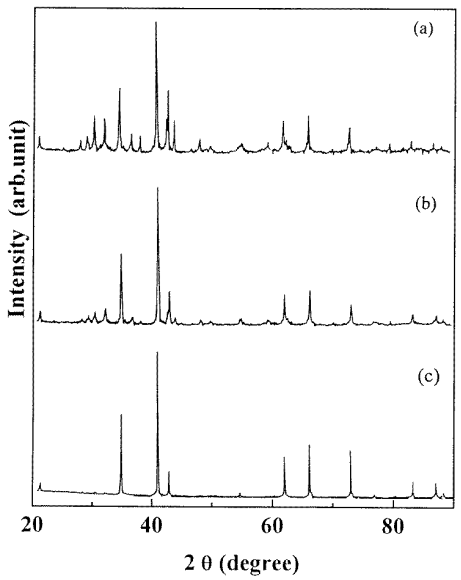

Figure 1. X-ray diffraction spectra of $Pr_{0.5}Ce_{0.5}Fe_2$ at different temperatures: (a) 850 °C, (b) 800 °C, (c) 700 °C.

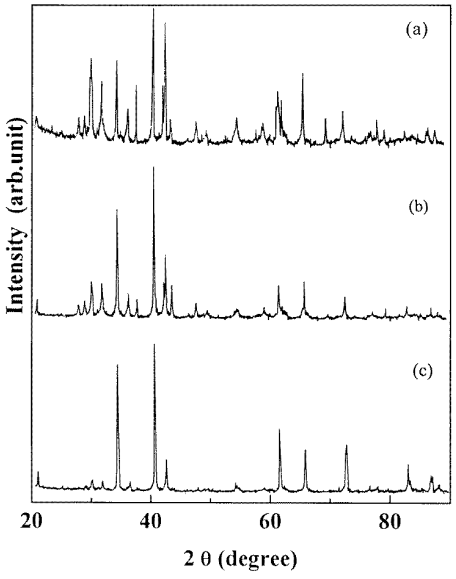

Figure 2. X-ray diffraction spectra of $Pr_{0.7}Ce_{0.3}Fe_2$ (nominal composition) at different temperatures: (a) 700 °C, (b) 800 °C, (c) 850 °C.

slight R_2Fe_{17} second phase. So the high annealing temperature above 850 °C is important for the synthesis of the Laves phase structure of high Pr concentration.

The lattice parameter dependence of Pr concentration for the pure phase obtained from x-ray diffraction is shown in figure 3. With the exception of $x = 0.3$ and $x = 0.4$ a linear increase is found with Pr concentration from $x = 0.0$ to 0.5. The exception can be ascribed to the change of Ce mixed-valence behaviour (see the discussion below). The $CeFe_2$ lattice parameter (7.301 Å) is slightly larger than the previously reported values (7.298 Å [8], 7.286 Å [9]).

Vegard's law describes the linear dependence of lattice parameter on the Pr concentration x in $Pr_xCe_{1-x}Fe_2$:

$$a = xa_1 + (1 - x)a_2 \tag{3.1}$$

where a_1 and a_2 are lattice parameters of $PrFe_2$ and $CeFe_2$, respectively. By fitting the line in figure 3 (except for $x = 0.3$ and $x = 0.4$) the lattice parameter of $PrFe_2$ will be 7.459 Å, that is close to the reported 7.467 Å of $PrFe_2$ synthesized at high pressure [3].

3.2. Magnetization and anisotropy constant

Magnetization curves at a temperature of 1.5 K for those samples with $x \leqslant 0.5$ are shown in figure 4. It can be seen that approximate saturation was achieved for all six samples of $x \leqslant 0.5$, hence it is possible to fit magnetization curves by an 'approximate saturation law':

$$M = M_s\left(1 - a/H - b/H^2 - c/H^3 - \ldots\right) + \chi_p H \tag{3.2}$$

where M_s is the spontaneous magnetization, a, b, c are fitting parameters, H is magnetic field and χ_p is parallel (paramagnetic) susceptibility. Because the temperature and magnetic

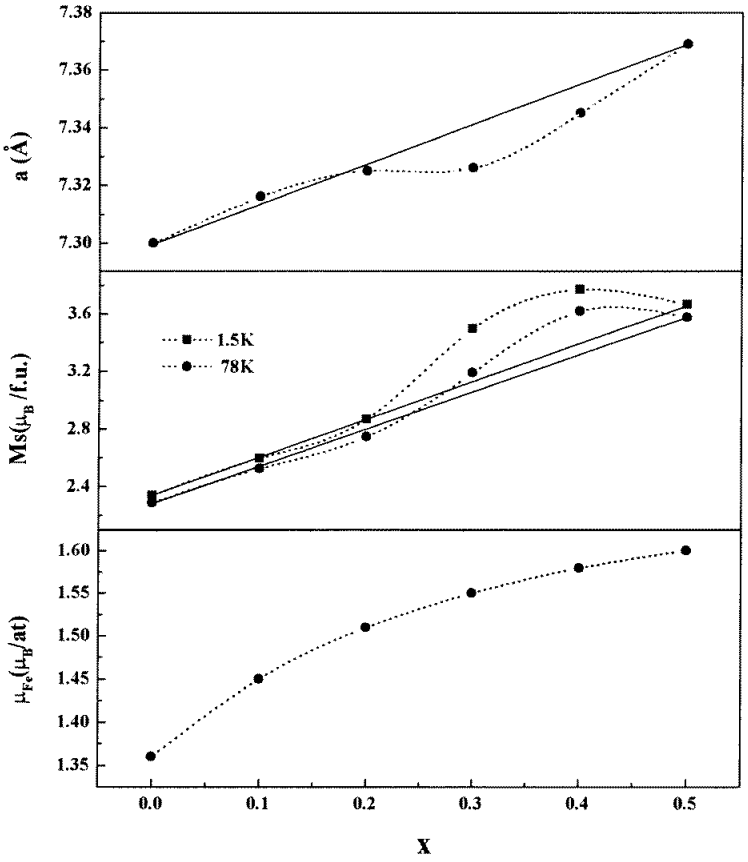

Figure 3. The variation with Pr concentration of $Pr_xCe_{1-x}Fe_2$ ($x \leqslant 0.5$) in lattice parameter at room temperature, spontaneous magnetic moment at 1.5 and 78 K and Fe local magnetic moment at 78 K from Mössbauer measurements. The solid lines represent the theoretical curves and points denote the experimental data. The broken lines are visual guides.

field variation of χ_p can be described by $TH^{-1/2}$ (T is temperature), $\chi_p H^{1/2}$ is regarded as a fitting parameter. For a cubic structure the relation of b and K_1 is simple:

$$b = 8K_1^2/105M_s^2\mu_0^2. \tag{3.3}$$

The available experimental results indicate that the easy magnetization axes (EMAs) of $PrFe_2$ [10] and $CeFe_2$ [11] are $\langle 100 \rangle$ at 1.5 and 78 K, and the EMA of $Pr_xCe_{1-x}Fe_2$ can also be regarded as $\langle 100 \rangle$ and K_1 must have a positive value. The fitting results are shown in figure 4.

M_s at temperatures of 1.5 and 78 K are listed in table 1. The spontaneous magnetic moment of $CeFe_2$ is 2.34 μ_B fu^{-1} which is consistent with those in other works [8, 12]. M_s versus Pr concentration increases linearly except for $x = 0.3$ and $x = 0.4$ (see figure 3) at the temperatures of 1.5 and 78 K. Suppose the $Pr_xCe_{1-x}Fe_2$ system can be regarded as the overlap of two Laves phase structures $PrFe_2$ and $CeFe_2$, then by extrapolating the mentioned linear relation in figure 3 to $x = 1.0$, one can find that the magnetic moment of $PrFe_2$ is 4.98 μ_B fu^{-1} at 1.5 K and 4.67 μ_B fu^{-1} at 78 K. The value at 78 K is in good agreement with that of Shimotomai *et al* [10] who have reported a value of 4.7 μ_B fu^{-1}

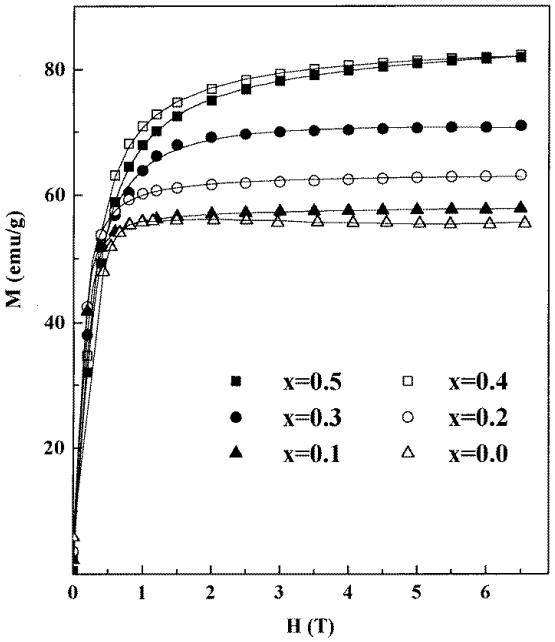

Figure 4. Magnetization isotherms of $Pr_xCe_{1-x}Fe_2$ ($x \leqslant 0.5$) at 1.5 K. The solid lines are fitting curves based on the approximate saturation law.

for high-pressure $PrFe_2$ at 78 K. The value at 1.5 K indicates ferromagnetic alignment of Pr and Fe moments.

Table 1. The lattice parameter (a), Curie temperature (T_C), spontaneous magnetic moment (M_s) and anisotropy constant (K_1) of $Pr_xCe_{1-x}Fe_2$ ($x \leqslant 0.5$).

			M_s (μ_B fu^{-1})		
x	a (Å)	T_C (K)	1.5 K	78 K	K_1 (10^5 J m^{-3})
0	7.301(1)	233(3)	2.34(2)	2.27(3)	0.73(6)
0.1	7.316(2)	300(3)	2.60(1)	2.52(4)	1.47(5)
0.2	7.325(1)	333(3)	2.87(2)	2.75(2)	1.64(5)
0.3	7.326(3)	364(3)	3.50(2)	2.19(3)	3.09(7)
0.4	7.349(5)	393(3)	3.77(4)	3.62(3)	2.98(6)
0.5	7.369(3)	415(3)	3.66(3)	3.57(2)	3.53(7)

The K_1 value of $Pr_xCe_{1-x}Fe_2$ increases rapidly with Pr concentration. In general, the magnetocrystalline anisotropy of the rare-earth–iron intermetallic compound results mainly from the rare-earth sublattice with the exception of $CeFe_2$. For $CeFe_2$, because the Ce 4f electrons transfer to the conduction band and the orbital momentum almost quenches, the magnetic-anisotropy behaviour is mainly due to Fe–Fe interaction. In the system of $Pr_xCe_{1-x}Fe_2$, the increased K_1 could be understood as the increase of Pr concentration. Roughly extrapolating the increase trends, the K_1 of $PrFe_2$ would possess an order of 7.3×10^5 J m^{-3}, which is even smaller than that of $TbFe_2$ (-7.6×10^6 J m^{-3}) and $DyFe_2$ (2.1×10^6 J m^{-3}) at room temperature [13].

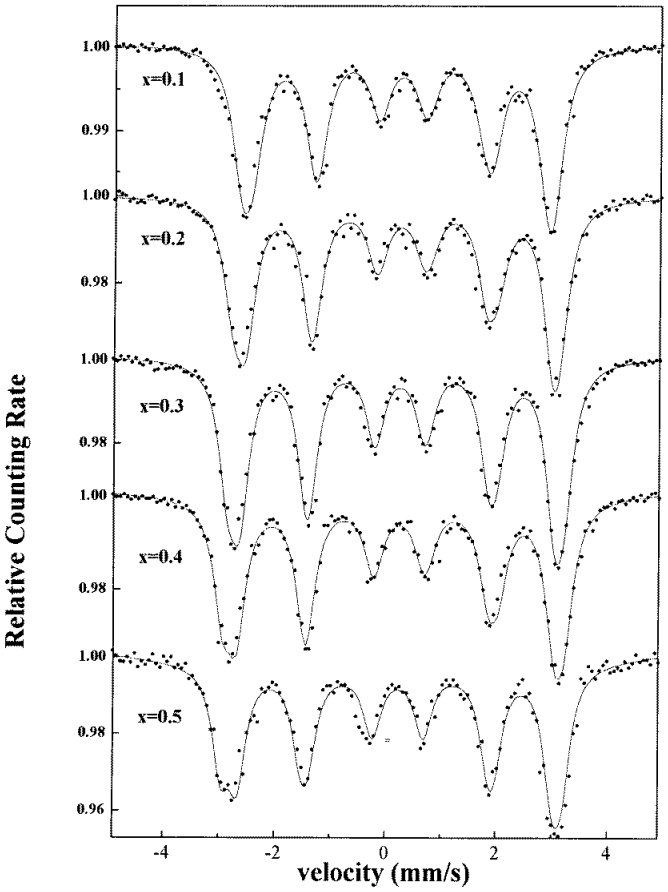

Figure 5. ^{57}Fe Mössbauer spectra of $Pr_xCe_{1-x}Fe_2$ (x from 0.5 to 0.9) at 78 K. The solid lines are computed fits.

3.3. Mössbauer spectra and Fe–Fe interaction

^{57}Fe Mössbauer spectra for single-phase $Pr_xCe_{1-x}Fe_2$ obtained at a temperature of 78 K are shown in figure 5. The spectrum of $CeFe_2$ is the simple six-line pattern with the 3:2:1 intensity ratio and indicates the presence of one single magnetically inequivalent iron site. With the increase of Pr concentration, those spectra at this temperature appear as a superposition of two six-line patterns.

For RFe_2 compounds with Laves phase structure, the number of six-line patterns (magnetically inequivalent irons) depends on the direction of the magnetic hyperfine field H_{eff} with respect to the cubic axis. The spectrum for an EMA of ⟨111⟩ consists of two six-line patterns with population ratio 3:1 [11]. However, in the present case, the superposition of two six-line patterns cannot be ascribed to the hyperfine field along the ⟨111⟩ direction because the intensity ratio of the two six-line patterns is not 3:1 or 2:2. Additionally the EMA of the investigated compound is ⟨100⟩ at 78 K: for $PrFe_2$ the EMA rotation from ⟨100⟩ to ⟨111⟩ occurs at a temperature between 164 and 195 K [10], and for $CeFe_2$ this process occurs at a temperature around 150 K [11]. The superposition might be due to the

loss of cubic symmetry, and the magnetostrictive effects in this compound might lead to a non-negligible departure from the cubic symmetry. Another possibility might be attributed to the contribution from the different rare-earth site ions because the ligand electric field gradient (EFG) tensor at iron sites results partly from the quadrupolar moment of the unfilled 3d shell and partly from that of the surrounding charges (4f electrons); especially in Ce-based Laves phase compounds the behaviour of the Ce ion is notably different from the other rare-earth elements. It has been reported that the hyperfine field at liquid-helium temperature is 193 kOe for $PrFe_2$ [10] and 156 kOe for $CeFe_2$ [11]. Our fitting results are in agreement with these values (see table 2). It is also worth noticing that the isomer shifts of the two six-line patterns are almost the same but the quadrupolar splittings (QS) have a notable difference.

Table 2. The hyperfine field H_{eff}, isomer shift (IS) and quadrupole splitting (QS) derived from ^{57}Fe Mössbauer spectra of $Pr_xCe_{1-x}Fe_2$. The last two columns represent the Fe local magnetic moment from two subspectra and average Fe magnetic moment.

	IS (mm s^{-1})		QS (mm s^{-1})		H_{eff} (kOe)		μ_{Fe} (μ_B/at)		
x	I	II	I	II	I	II	I	II	μ_{Fe} (μ_B/at)
0	0.21(1)		0.06(1)		156(1)		1.36(1)		1.36(1)
0.1	0.20(2)	0.21(2)	0.05(1)	0.13(1)	165(2)	176(1)	1.43(2)	1.53(1)	1.45(2)
0.2	0.19(2)	0.22(1)	0.06(2)	0.15(2)	171(2)	182(3)	1.49(2)	1.58(3)	1.51(2)
0.3	0.19(2)	0.20(1)	0.02(2)	0.10(2)	175(4)	187(2)	1.52(4)	1.63(2)	1.55(4)
0.4	0.18(3)	0.20(2)	0.03(2)	0.14(1)	177(3)	190(3)	1.54(3)	1.65(3)	1.58(3)
0.5	0.17(2)	0.16(2)	0.07(3)	0.11(3)	177(3)	192(4)	1.54(3)	1.67(4)	1.60(3)

On the basis of the latter assumption, the Fe hyperfine field is expressed as the weighted average hyperfine field of two six-line subspectra corresponding to $CeFe_2$ and $PrFe_2$, respectively. The details of Mössbauer parameters are listed in table 2. The approximate relationship between hyperfine field H_{eff} and Fe local magnetic moment μ_{Fe} has been found to work well for many intermetallic compounds: $H_{eff} = A_{hf}\mu_{Fe}$. Taking into account that the hyperfine field of $CeFe_2$ is 165 kOe at 4.2 K and $\mu_{Fe} = 1.43\ \mu_B$, It is reasonable to take $A_{hf} = 115$ kOe μ_B^{-1} that is smaller than that of normal rare-earth–iron intermetallic compounds, in which the selected value is 145 kOe μ_B^{-1}. The magnetic moment μ_{Fe} versus Pr concentration is also shown in figure 3. It can be seen that the local magnetic moment increases with Pr concentration. The Curie temperature of $Pr_xCe_{1-x}Fe_2$, shown in figure 6, also increases with increasing x. The increase indicates that Fe–Fe interaction is enhanced with the increase of Pr concentration.

3.4. Magnetostriction

Magnetostriction curves were measured at room temperature as shown in figure 7. All samples exhibit the anisotropy magnetostriction and the largest saturation magnetostriction λ_s is about 200 ppm occuring at $x = 0.5$. It can be seen clearly that the magnetostriction increases rapidly with the substitution of Pr for Ce. Magnetostriction is thought to result mainly from the contribution of the rare-earth sublattice in the RFe_2 structure, and those rare-earth ions are localized and exhibit trivalence. The cerium ion in $CeFe_2$ shows mixed-valence behaviour and does not possess magnetostriction. Consequently the linear increase of magnetostriction is only due to the increase of Pr concentration.

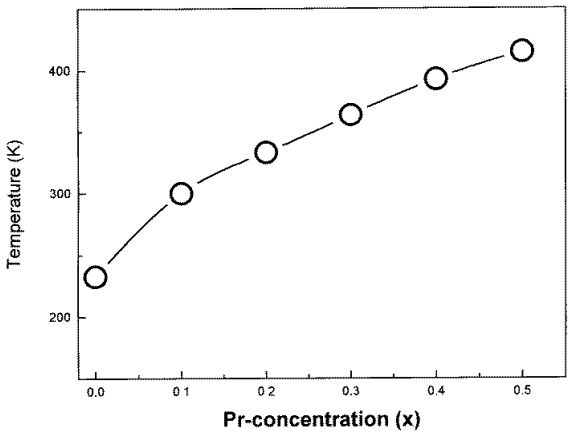

Figure 6. Curie temperature dependence on Pr concentration in $Pr_xCe_{1-x}Fe_2$.

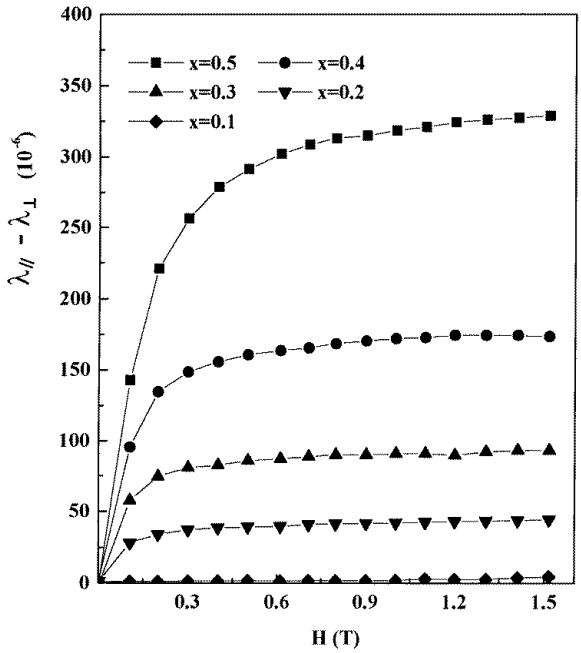

Figure 7. Magnetostriction isotherms of $Pr_xCe_{1-x}Fe_2$ at room temperature.

4. Discussion

The formation of $Pr_xR_{1-x}Fe_2$ (R = Sm [14], Tb [15]) has been reported and the Pr concentration does not exceed $x = 0.35$ for Sm and $x = 0.2$ for Tb at most, otherwise a second phase occurs. In this study Pr concentration has been successfully extended to $x = 0.5$ with the substitution of Ce. It is worth noticing that the Sm ion has stronger 4f bonding than that of Tb although its atom radius is larger than that of the latter. Additionally the cerium ion possesses the strongest 4f bonding among all the rare-earth ions. All the facts

seem to suggest that the large 4f bonding of rare-earth elements can be a very important factor in synthesizing this type of Pr-based pseudo-binary structure.

A valence change of the Ce ion can be found in the investigated system $Pr_xCe_{1-x}Fe_2$. The same change is also observed in the $Ce_xDy_{1-x}Fe_2$ system which will be published later. However the latter changes from mixed-valence state to trivalent or 'nearly trivalent'; in $Pr_xCe_{1-x}Fe_2$ the change is toward tetravalent at a specific range from $x = 0.2$ to $x = 0.5$. The result can be verified from the following aspects.

(A) *The anomaly of lattice parameter.* Figure 3 shows the anomalous points $x = 0.3$ and $x = 0.4$ that disobey Vegard's law. The decrease of parameter in this range can be thought to result from the tendency of Ce toward tetravalence because the radius of the Ce ion decreases with the weakness of the degree of localization of Ce.

(B) *The anomaly of spontaneous magnetic moment.* In the mentioned range the spontaneous magnetic moment deviates from the excellent linear dependence. Within the magnetic sublattice model, because the moments from Pr and Fe sublattice couple ferromagnetically and the Ce moment couples ferrimagnetically with the Fe moment, the observed spontaneous moment can express as $\mu_{Pr} + \mu_{Fe} - \mu_{Ce}$. It can be seen from figure 3 that μ_{Fe} does not vary abnormally in this range. Therefore the anomalous increase can be ascribed to the decrease of Ce moment only, i.e., the valence changes toward tetravalent.

In conclusion, the substitution of Ce for Pr in $Pr_xCe_{1-x}Fe_2$ is conducive to the formation of the Pr-based Laves phase compound. Appropriate annealing conditions can extend Pr concentration up to $x = 0.8$ in synthesizing the pseudo-binary compound at ambient pressure and a pure Laves phase exists at least up to $x = 0.5$. This should be ascribed to the strong 4f bonding of the Ce ion in the intermetallic compound. The Fe–Fe interaction, Curie temperature and magnetostriction increase with increasing Pr concentration. In a specific range lattice parameter and spontaneous magnetization anomalies exist that can be attributed to the change of Ce ion valence toward tetravalent.

References

[1] Clark A E 1980 *Ferromagnetic Materials* vol 1, ed E P Wohlfarth (Amsterdam: North-Holland)
[2] Laves F 1939 *Naturwiss* **27** 65
[3] Cannon J F, Robertson D L and Hall H T 1972 *Mater. Res. Bull.* **7** 5
[4] Meyer C, Hartmann-Boutron F, Gros Y, Berthier Y and Capponi B 1979 *J. Physique Coll.* **40** C5 191
[5] Meyer C, Hartmann-Boutron F, Gros Y, Berthier Y and Buevoz J L 1980 *J. Physique* **42** 605
[6] Mori T and Uchida T 1992 *IEEE Trans. Magn.* **MAG-28** 3165
[7] Kida G, Nakagawa Y, Nishihara Y and Iga Y 1990 *J.Magn. Magn. Mater.* **90/91** 75
[8] Cunda S F, Guimaraes A P and Livi F P 1980 *J. Phys. Chem. Solids* **41** 761
[9] Mansey R C, Raynor G V and Harris I R 1968 *J. Less-Common Met.* **14** 329
[10] Shimotomai M, Miyake H and Doyama M 1980 *J. Phys. F: Met. Phys.* **10** 707
[11] Atzmony U and Dariel M P 1974 *Phys. Rev.* B **10** 2060
[12] Eriksson O, Nordstrom L, Brooks M S S and Johansson B 1988 *Phys. Rev. Lett.* **60** 2523
[13] Clark A E 1974 *AIP Conf. Proc.* **18** 1015
[14] Shimotomai M and Doyama M 1983 *J. Magn. Magn. Mater.* **31–34** 215
[15] Clark A E, Abbundi R, McMasters O and Savage H 1977 *Physica* B **83** 86